



Rheological and electrical analysis in carbon nanofibre reinforced polypropylene composites

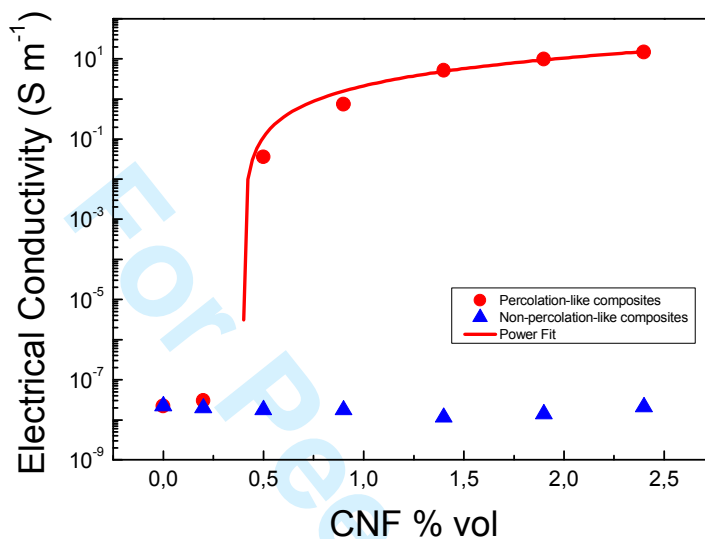
Journal:	<i>Journal of Polymer Science Part B: Polymer Physics</i>
Manuscript ID:	Draft
Wiley - Manuscript type:	Full Papers
Date Submitted by the Author:	n/a
Complete List of Authors:	Paleo, Antonio; University of Minho, IPC – Institute for Polymers and Composites Silva, Jorge; Case Western Reserve University, Dept. of Macromolecular Science and Engineering Hattum, Ferrie; Institute for Polymers and Composites, Lanceros-Mendez, Senentxu; University of Minho - Campus de Gualtar, Department of Physics; Ares, Ana; University of A Coruña, Grupo de Polímeros. Departamento de Física
Keywords:	nanocomposites, rheology, conductive network, extrusion

SCHOLARONE™
Manuscripts

view

Rheological and electrical analysis in carbon nanofibre reinforced polypropylene composites

A. J. Paleo, J. Silva, F. W. J. van Hattum, S. Lanceros-Méndez and A. I. Ares



Two different carbon nanofibers were incorporated in in the same polypropylene by twin-screw extrusion. Electrically, the two carbon nanofiber based composites demonstrated to have different response: non-conducting and conducting as a function of volume fraction concentration. A large difference in the rheological behavior of both composites has been measured. Furthermore, after comparing electrical conductivity and rheological analysis, it is concluded that G' / G'' is the most appropriate rheological parameter for comparing with electrical behavior.

Authors: *A. J. Paleo, J. Silva, F. W. J. van Hattum, S. Lanceros-Méndez and A. I. Ares*

Title: *Rheological and electrical analysis in carbon nanofibre reinforced polypropylene composites*

Affiliations and address:

Antonio J. Paleo and F. W. J. van Hattum

IPC – Institute for Polymers and Composites, University of Minho, Campus de Azurém,
4800-058 Guimarães, Portugal

J. Silva

Dept. of Macromolecular Science and Engineering, Case Western Reserve University, CLiPS
- Center for Layered Polymeric Systems, Kent Hale Smith Bldg., Room # 341 2100 Adelbert
Rd.

Cleveland, OH 44106-7202, USA

Senentxu Lanceros-Méndez

Center/Department of Physics, University of Minho, Campus de Gualtar, 4710-057 Braga,
Portugal

A. I. Ares

Grupo de Polímeros. Departamento de Física. Universidade de A Coruña. Laboratorio de
Polímeros. E.U.P. Avda 19 Febrero, s/n 15405- Ferrol, España.

Corresponding author:

Antonio J. Paleo

Telephone : (+351) 253510320

fax : (+351) 253510339

e-mail : antonio.vieito@dep.uminho.pt

ABSTRACT

Two different types of carbon nanofibers (CNF) were incorporated in the same polypropylene (PP) matrix by twin-screw extrusion. The electrical characterization of both CNFs / PP composites as a function of volume fraction show different electrical performance: conducting and non-conducting. The objective of this work is to study the rheological behaviour of both composites with the aim of relating it to the electrical behaviour. The results indicate that the rheological behaviours are different, suggesting that rheology differentiates the microstructural variations responsible for the electrical performance. Furthermore, the main rheological parameters were correlated to the electrical conductivity. The results show that G'/G'' and G' are the most sensitive parameters when compared to the onset of electrical percolation. Finally, in spite of the intrinsic measuring differences between electrical and rheological analysis, the two calculated thresholds are very similar: ~ 0.5 for the rheological and ~ 0.4 for the electrical.

KEYWORDS polypropylene, carbon nanofibers, electrical conductivity, rheological parameters, percolation

INTRODUCTION

Several nanostructures composed of graphitic layers, including nanographene platelets (NGPs), carbon nanofibers (CNFs) and nanotubes (CNTs) are currently the focus of intense investigation. CNFs in particular have a unique morphology in which exposed graphene edge planes are placed on the outer surface of the fiber.¹ Their outer diameter, which ranges from 50 to 200 nm, is slightly larger than CNTs. The inner diameters and lengths range from 30 to 90 nm and from 50 to 100 μm , respectively.^{2,3} Furthermore, their excellent electrical, thermal and mechanical characteristics as well as their simple incorporation and dispersion into polymers at a lower cost in comparison to carbon nanotubes, have converted CNFs into an object of study in several fields of materials science.^{4,5}

An important area of application of carbon nanofibers is in the field of composite materials. By incorporating relatively small loadings of CNFs in a polymer matrix, electrically

1
2
3
4
5
6
7
8
9
10
11
12
13
14
15
16
17
18
19
20
21
22
23
24
25
26
27
28
29
30
31
32
33
34
35
36
37
38
39
40
41
42
43
44
45
46
47
48
49
50
51
52
53
54
55
56
57
58
59
60

conductive composites can be produced, while at the same time increasing its mechanical properties. Some of the final uses of these CNFs based polymer composites are electrostatic dissipative (ESD), electromagnetic shielding (EMI) and radio frequency interference (RFI) materials.^{6,7}

Up to now, the majority of research in CNTs and CNFs based polymer composites has been motivated by the importance of several key-factors for the development of conducting and structural multifunctional materials: composites morphology, analysis of dispersion and distribution of nanofillers in the polymer, polymer-nanofiller interactions and the lowest loading required for conductive network formation.^{4,8-11}

Additionally, it has been commonly established that rheological analysis, besides being a method to study viscoelastic properties to assess processing behavior, provides insights on the interaction between carbon nanostructures and polymer in the melt state.^{12, 13} Kharchenko et. al characterized the transport property transitions in multiwall nanotubes (MWNT) dispersed in polypropylene (PP). In their study the electrical threshold (0.0025 volume fraction) precedes the rheological threshold (0.01 volume fraction), based on the rheological analysis of the inverse of loss tangent (G'/G'').¹⁴ By plotting G' as a function of nanotube loading in single-walled carbon nanotube (SWNT) / poly(methyl methacrylate) (PMMA) nanocomposites, Du et. al reported a rheological threshold of 0.12 wt %, whereas a value of 0.39 wt % was obtained for the electrical threshold. In this study, the onset of viscoelastic behavior was explained as the loading from which the distance between nanotube clusters is shorter than the size of the polymer chain causing restriction of polymer motion.¹² More recently, in their attempt to compare quantitatively electrical with rheological values in polystyrene (PS) containing MWCNTs, Kota et. al conclude that the storage modulus, G' , and G'/G'' , rheological parameters related to the elastic load transfer, are more sensitive to

1
2
3 the onset of electrical percolation than η^* and G'' , rheological parameters related to
4
5 dissipation mechanisms.¹⁵
6
7

8
9 Though several attempts to correlate conductivity with rheological properties have been
10
11 discussed in CNT based polymer nanocomposites, there are only few studies focused on the
12
13 investigation of percolation thresholds through electrical and rheological analysis of CNF
14
15 based polymer nanocomposites.¹⁶ Furthermore, to our knowledge, there is no investigation
16
17 evaluating rheological and electrical properties in electrical and non-electrical conducting
18
19 composites with the aim of discussing if rheological analysis allows distinguishing electrical
20
21 conducting from electrical isolating response in this kind of systems. Besides, in order to
22
23 compare electrical with rheological thresholds, the most sensitive rheological parameter is
24
25 calculated. The work has been performed with two different CNFs incorporated in the same
26
27 polypropylene (PP) matrix through twin-screw extrusion under the same processing
28
29 conditions.
30
31

32 33 **EXPERIMENTAL**

34 35 **Materials and Methods**

36
37 A PP powder, Borealis EE002AE, was used as polymer matrix. The two types of stacked-cup
38
39 CNFs used in this study (PR 24 LHT XT and PR 25 PS XT), commercially known as
40
41 Pyrograf IIITM, were supplied by Applied Sciences, Inc. (ASI, Cedarville, OH, USA).
42
43 Electrically conducting fibers, PR 24 LHT XT, in the form of a loose powder with a bulk
44
45 density of $\sim 1.95 \text{ g/cm}^3$ and a highly graphitic outer wall layer, have an average diameter of
46
47 80 nm. They have been heat-treated at temperatures of 1500 °C. Electrically conducting
48
49 fibers, PR 25 PS XT, with a bulk density of $\sim 0.032 \text{ g/cm}^3$ and an outer layer consisting on a
50
51 disordered pyrolytically stripped layer with a large number of graphitic edge sites available
52
53 along the length, have an average diameter of 120 nm.^{17,18} They have been heat-treated at
54
55
56
57
58
59
60

1
2
3 temperatures of 600 °C. Both types of CNFs had a debulking treatment in order to lower their
4
5 respective bulk densities.
6

7
8 PP/CNF nanocomposites were fabricated, under the same processing conditions, on a
9
10 modular lab-scale intermeshing mini-co-rotating twin-screw extruder, with a screw diameter
11
12 of 13 mm, barrel length of 31 cm and an approximate L / D ratio of 26, coupled to a
13
14 cylindrical rod die of approximate 2.85 mm of diameter. The extruded PP/CNF
15
16 nanocomposites were then pelletized and pressed into compression-moulded with the
17
18 appropriate geometries for electrical and rheological tests. A detailed description of the melt-
19
20 compounding conditions and machining of samples has been previously published.¹⁹
21
22

23
24 The nomenclature used to designate the composites is summarized in Table 1.
25
26

27 **Characterization**

28
29 Morphological characterization and CNF dispersion of the composites were examined using a
30
31 JEOL JSM-6400 scanning electron microscope (SEM) at an accelerating voltage of 20 kV.
32
33 The samples were broken under cryogenic conditions and then sputter-coated with a thin
34
35 layer of gold before testing.
36
37

38
39 Electrical characterization was performed by measuring the bulk resistance of ten rectangular
40
41 replicates per sample with an automated Keithley 487 picoammeter/voltage source and then
42
43 the total average was calculated. The samples' dimensions were 49 mm x 10 mm x 1 mm. All
44
45 the experiences were performed at room temperature in direct current (DC) by using the two-
46
47 probe method. The samples' extremities were painted with conductive silver paste. The
48
49 volume conductivity in $S\ m^{-1}$ was calculated taken into account the geometrical
50
51 characteristics of the samples.¹⁹
52
53

54
55 Viscoelastic characterization was performed using a controlled strain rheometer (ARES, TA
56
57 Instruments) with parallel-plate geometry (25 mm diameter, 2 mm gap) at 190 °C. Complex
58
59
60

1
2
3 viscosity (η^*), storage modulus (G'), loss modulus (G'') and inverse of loss tangent ($G' /$
4 G'') were measured as a function of frequency (ω). The rheological tests were performed in
5 the linear viscoelastic region (LVE) where the modulus is independent of strain. The linear
6 viscoelastic region was determined by a strain sweep before testing the viscoelasticity of the
7 composites under a frequency test. At the end, frequency sweep measurements were set up in
8 the frequency range from 1×10^{-1} to 10^2 rad/s.
9
10
11
12
13
14
15
16

17 **RESULTS AND DISCUSSION**

18 **Morphological analysis**

19
20 The SEM observations of the 1.9 % vol CNFs filled nanocomposites demonstrate that the two
21 composites reveal different structures. PR 24 LHT XT composites, electrically conducting for
22 1.9 % vol loading, show that CNFs are well dispersed, distributed and close enough to each
23 other, Figure 1(a). PR 25 PS XT composites, in opposite, though show also well distributed
24 and dispersed morphology, exhibit a larger distance between fibers for the same loading of
25 1.9 % vol. This fact suggests the need of a larger content of CNFs to provide electrical
26 conductive composites, Figure 1(b).
27
28
29
30
31
32
33
34
35
36

37 **Electrical properties in CNFs / PP nanocomposites**

38
39 The electrical volume conductivity of the neat PP and CNF/PP composites as a function of
40 CNF concentration is represented in Figure 2. Each data point on the plot represents the
41 average of 10 samples. Pure PP has an electrical conductivity of $2.22 \times 10^{-8} \text{ S m}^{-1}$. PR 24
42 LHT XT composites increased by 9 orders of magnitude, approaching a value of 14.9 S m^{-1}
43 for 2.4 % vol loading, whereas PR 25 PS XT composites showed no relevant increase of the
44 electrical conductivity for all filler loadings. The heat treatment at temperatures of $1500 \text{ }^\circ\text{C}$ of
45 PR 24 fibres (LHT grade) with a more ordered structure on the fiber's surface and better
46 intrinsic conductivity, together with the higher bulk density which allows better distribution
47
48
49
50
51
52
53
54
55
56
57
58
59
60

1
2
3 and dispersion in the PP, unlike PR 25 fibers, demonstrate superior electrical conducting
4
5 results for this particular polymer and processing method.²⁰
6
7

8 The variation of the transport properties with dispersion state of carbon-based
9
10 nanocomposites is usually understood in the framework of the percolation theory.²¹⁻²³
11
12 According to this, the behavior of the conductivity can be described by the following power
13
14 law relation:
15
16

$$\sigma \propto (\phi - \phi_c)^t \quad (1)$$

17
18
19
20 where σ is the electrical conductivity, t is a critical exponent, Φ_c the critical volume fraction
21
22 and Φ the filler volume fraction. Experimental percolation threshold for PR 24 LHT XT
23
24 composites is bounded between ~0.2 and ~0.5 % vol, as shown in Figure 2. More precisely,
25
26 by means of equation 1, a value of 0.42 % vol \pm 0,07 is obtained. The critical exponent value
27
28 ~1,75 is in agreement with the theoretical 3D values. The critical exponent points out that the
29
30 conductivity is related to the formation of a 3D network that spans the system, whereas the
31
32 experimental values of percolation threshold represent a deviation from theoretical prediction
33
34 associated to the existence of small agglomerates, as previously discussed.¹⁹
35
36
37
38

39 **Rheological properties in CNFs / PP nanocomposites**

40
41
42 The frequency dependence of the shear storage modulus G' , the loss modulus G'' , inverse of
43
44 the loss tangent G'/G'' , and complex viscosity η^* , for the two composites with different
45
46 loadings of CNF, at the temperature used during the extrusion, i. e., 190 °C, are shown in
47
48 Figures 3, 4, 5 and 6, respectively. Several common features can be observed. First, a
49
50 reduction for the two lowest loadings 0.2 and 0.5 % vol compared with the neat PP is
51
52 observed in all rheological properties. In this regard, the CNFs may act as nucleating agents
53
54 for PP and make the polymer chains to be well aligned and ordered. However, for higher
55
56
57
58
59
60

1
2
3 loadings, the surface available for nucleating is huge and there are not enough polymer chains
4
5 to go and crystallize on the fibers.²⁴
6
7

8 The filled composites and the neat PP exhibit similar results due to shear-thinning effect in
9
10 the high frequency region.²⁵ Overall, it is accepted that, at low frequencies, viscoelastic
11
12 behavior shows information about the formation of fibers' networks at a certain levels of
13
14 reinforcement,¹² while at high frequencies the rheological analysis reflects motions of short
15
16 molecular chains independently of filler.²⁶
17
18

19
20 Particularly in Figure 3, the storage modulus, G' , which provides a measure of "stiffness",²⁷,
21
22 ^{12, 14} is compared for all composites as a function of frequency. For PP / PR 24 LHT XT
23
24 composites, Figure 3(a), for a frequency of 0.1 rad/s, G' exhibits an abrupt change in
25
26 modulus between 0.5 and 0.9 % vol with values of 21 and 860 Pa, respectively, with a
27
28 maximum of 15411 Pa for 2.4 % vol. A total increase of three orders of magnitude therefore.
29
30 This point indicates the creation of a continuous filler's network which restrains the long-
31
32 range motions of the polymer chains.²⁶ In addition, at loadings higher than 0.5 % vol, the G'
33
34 is clearly less dependent on frequency than for lower volume fractions. This particular
35
36 response is associated with the transition from liquid-like to solid-like viscoelastic behavior.¹²
37
38
39

40
41 It has been discussed in previous studies that dispersion plays a key role in the viscoelastic
42
43 properties of CNT/polymer nanocomposites. In this study, PP / PR 24 LHT XT composites
44
45 demonstrate to have a low-frequency slope of G' at the highest loadings of CNFs, which has
46
47 been associated to good dispersion.¹²
48
49

50
51 PP / PR 25 PS XT composites, on other hand, do not reveal significant changes in behavior
52
53 compared to pure PP, Figure 3(b). Further, a modest increase of modulus with a maximum of
54
55 173 Pa for 2.4 % vol loading is observed for 0.1 rad/s. According to the above discussion,
56
57 this behavior together with the frequency dependence of G' for all volume fractions may
58
59
60

1
2
3 indicate that PP / PR 25 LHT XT composites have not formed yet an interconnected structure
4
5 even at the maximum loading of 2.4 % vol.
6
7

8 The loss modulus, G'' , which provides a measure of viscous resistance to deformation, as a
9
10 function of frequency, is shown in Figure 4. Consistently with storage modulus, at low
11
12 frequencies G'' increases with increasing CNF content for all composites, with exception of
13
14 the two lowest loading contents of CNF 0.2 and 0.5 % vol. On the other hand, the increase in
15
16 G'' is lower than the storage modulus G' at a fixed CNF content. This lower behavior was
17
18 already reported.^{26, 27} Again, the increase is more pronounced for PP / PR 24 LHT XT
19
20 composites, which above a content of 0.9 % vol show a clear change in behavior compared to
21
22 pure PP. This last circumstance is not observed for PP / PR 25 PS XT composites, which
23
24 suggests that there is no evidence of interconnected nanofiber's networks.
25
26
27

28
29 Supplementary information about interaction between CNFs and the polymer can also be
30
31 estimated through the inverse loss tangent (G''/G'), Figure 5, which relates elastic (G') with
32
33 dissipative (G'') characteristics of the composites.¹⁴ The curves follow the same trend of G'
34
35 and G'' . Nevertheless, it is important to highlight the sharp variation between 0.5 and 0.9 vol
36
37 %, as it happens with G' for the same content of CNF, in PP / PR 24 LHT XT composites.
38
39

40
41 The frequency dependence of the complex viscosity, η^* , for the PP / CNFs nanocomposites is
42
43 shown in Figure 6. The pure PP shows a Newtonian plateau at low frequencies, whereas for
44
45 PP / PR 24 LHT XT composites, from 0.5 % vol the plateau decreases and yield stress
46
47 appears, consistently with behaviors observed for G' and G'' .
48
49

50
51 PP / PR 25 LHT XT composites, although show a clear variation in value of η^* between 0.9
52
53 and 1.4 % vol, do not change apparently the shape of the curve.
54
55
56
57
58
59
60

1
2
3 Summarizing the quantitative assessment of the experimental rheological analysis, depending
4 on the type of carbon nanofiber substantial differences can be appreciated between the two
5 composites. PP / PR 24 LHT XT composites, consistently with theoretical predictions and
6 previous experimental reports in CNTs based polymer composites, show a transition between
7 liquid-like and solid-like: as the nanofiber content increases, the creation of some
8 interconnected structure leads to a solid-like behavior ($G' > G''$), which explain the plateaus
9 or independence behavior with frequency for G' and G'' at the lower frequencies.^{27, 29}

19 **Comparison of electrical and rheological behaviors in CNFs / PP nanocomposites**

20 Electrical and rheological correlations may constitute a route to understand composites'
21 microstructure.
22
23

24
25
26 According to the electrical results, PR 24 LHT XT composites exhibit an abrupt transition
27 from isolating to electrical conducting behavior, which can be described in the context of
28 percolation theory, from contents of CNFs of ~ 0.42 % vol. In terms of microstructure, this
29 fact is related to the formation of a 3D CNFs' network which allows electrical transport. PR
30 25 LHT XT composites, on their hand, do not show isolating-to-conducting electrical
31 transition.
32
33

34
35
36 First, in order to calculate the most appropriate rheological parameter to describe rheological
37 thresholds, the normalized logarithm values of G' , G'' , G' / G'' and η^* are plotted and
38 compared with the normalized logarithm values of electrical conductivity for PR 24 LHT XT
39 composites in Figure 7.¹⁵ Though G' is commonly reported as the most adequate rheological
40 parameter to describe rheological thresholds, up to now this question is still under discussion
41 and different assumptions have been reported in the literature: power-law dependence based
42 on G' ,^{15, 12, 30} power-law dependence based on G' / G'' ,^{14, 15} and even on η^* .³¹ In Figure 7,
43
44
45
46
47
48
49
50
51
52
53
54
55
56
57
58
59
60
61
62
63
64
65
66
67
68
69
70
71
72
73
74
75
76
77
78
79
80
81
82
83
84
85
86
87
88
89
90
91
92
93
94
95
96
97
98
99
100
101
102
103
104
105
106
107
108
109
110
111
112
113
114
115
116
117
118
119
120
121
122
123
124
125
126
127
128
129
130
131
132
133
134
135
136
137
138
139
140
141
142
143
144
145
146
147
148
149
150
151
152
153
154
155
156
157
158
159
160
161
162
163
164
165
166
167
168
169
170
171
172
173
174
175
176
177
178
179
180
181
182
183
184
185
186
187
188
189
190
191
192
193
194
195
196
197
198
199
200
201
202
203
204
205
206
207
208
209
210
211
212
213
214
215
216
217
218
219
220
221
222
223
224
225
226
227
228
229
230
231
232
233
234
235
236
237
238
239
240
241
242
243
244
245
246
247
248
249
250
251
252
253
254
255
256
257
258
259
260
261
262
263
264
265
266
267
268
269
270
271
272
273
274
275
276
277
278
279
280
281
282
283
284
285
286
287
288
289
290
291
292
293
294
295
296
297
298
299
300
301
302
303
304
305
306
307
308
309
310
311
312
313
314
315
316
317
318
319
320
321
322
323
324
325
326
327
328
329
330
331
332
333
334
335
336
337
338
339
340
341
342
343
344
345
346
347
348
349
350
351
352
353
354
355
356
357
358
359
360
361
362
363
364
365
366
367
368
369
370
371
372
373
374
375
376
377
378
379
380
381
382
383
384
385
386
387
388
389
390
391
392
393
394
395
396
397
398
399
400
401
402
403
404
405
406
407
408
409
410
411
412
413
414
415
416
417
418
419
420
421
422
423
424
425
426
427
428
429
430
431
432
433
434
435
436
437
438
439
440
441
442
443
444
445
446
447
448
449
450
451
452
453
454
455
456
457
458
459
460
461
462
463
464
465
466
467
468
469
470
471
472
473
474
475
476
477
478
479
480
481
482
483
484
485
486
487
488
489
490
491
492
493
494
495
496
497
498
499
500
501
502
503
504
505
506
507
508
509
510
511
512
513
514
515
516
517
518
519
520
521
522
523
524
525
526
527
528
529
530
531
532
533
534
535
536
537
538
539
540
541
542
543
544
545
546
547
548
549
550
551
552
553
554
555
556
557
558
559
560
561
562
563
564
565
566
567
568
569
570
571
572
573
574
575
576
577
578
579
580
581
582
583
584
585
586
587
588
589
590
591
592
593
594
595
596
597
598
599
600
601
602
603
604
605
606
607
608
609
610
611
612
613
614
615
616
617
618
619
620
621
622
623
624
625
626
627
628
629
630
631
632
633
634
635
636
637
638
639
640
641
642
643
644
645
646
647
648
649
650
651
652
653
654
655
656
657
658
659
660
661
662
663
664
665
666
667
668
669
670
671
672
673
674
675
676
677
678
679
680
681
682
683
684
685
686
687
688
689
690
691
692
693
694
695
696
697
698
699
700
701
702
703
704
705
706
707
708
709
710
711
712
713
714
715
716
717
718
719
720
721
722
723
724
725
726
727
728
729
730
731
732
733
734
735
736
737
738
739
740
741
742
743
744
745
746
747
748
749
750
751
752
753
754
755
756
757
758
759
760
761
762
763
764
765
766
767
768
769
770
771
772
773
774
775
776
777
778
779
780
781
782
783
784
785
786
787
788
789
790
791
792
793
794
795
796
797
798
799
800
801
802
803
804
805
806
807
808
809
810
811
812
813
814
815
816
817
818
819
820
821
822
823
824
825
826
827
828
829
830
831
832
833
834
835
836
837
838
839
840
841
842
843
844
845
846
847
848
849
850
851
852
853
854
855
856
857
858
859
860
861
862
863
864
865
866
867
868
869
870
871
872
873
874
875
876
877
878
879
880
881
882
883
884
885
886
887
888
889
890
891
892
893
894
895
896
897
898
899
900
901
902
903
904
905
906
907
908
909
910
911
912
913
914
915
916
917
918
919
920
921
922
923
924
925
926
927
928
929
930
931
932
933
934
935
936
937
938
939
940
941
942
943
944
945
946
947
948
949
950
951
952
953
954
955
956
957
958
959
960
961
962
963
964
965
966
967
968
969
970
971
972
973
974
975
976
977
978
979
980
981
982
983
984
985
986
987
988
989
990
991
992
993
994
995
996
997
998
999
1000

1
2
3 above, the normalized logarithm values of G'' and η^* show a gradual increase with
4 concentration when compared with G' and mainly with G'/G'' which demonstrates to be the
5 most sensitive parameter to the rheological thresholds and the most adequate parameter for
6 comparing with electrical conducting values from 0.9 % vol. This is in accordance with the
7 study by Kharchenko et. al, which uses the inverse of loss tangent to compare with electrical
8 conductivity,¹⁴ and the study by Kota et. al, which concludes that η^* and G'' , related to
9 viscous response, are less sensitive than G' and G'/G'' , related to the elastic response.¹⁵
10
11
12
13
14
15
16
17
18

19 In order to compare the rheological and electrical thresholds, a power-law was fitted to G'/G''
20 G'' and G' . The equations used and the two rheological parameters, together with the
21 determined values of σ , are listed in Table 2. As it can be seen, the rheological threshold
22 based on G'/G'' analysis is ~ 0.49 % vol whereas for G' is ~ 0.47 % vol, which indicates that
23 the rheological threshold occurs at a slight higher concentration than the electrical percolation
24 threshold (0.42 % vol $\pm 0,07$). The different values obtained for rheological and electrical
25 thresholds in literature are cause of discussion. Some studies show that rheological threshold
26 occurs after electrical percolation, referring that connectivity between fibers precedes rigidity
27 percolation of the system.¹⁴ Others studies, nevertheless, point out the opposite, on the basis
28 of an adequate combination of alignment, dispersion of the fillers and molecular weight of
29 polymer matrix.¹²
30
31
32
33
34
35
36
37
38
39
40
41
42
43

44 The exponents calculated on the basis of a normal power law relation, were 0.52 for G'/G''
45 and 1.54 for G' . Even though for the electrical percolation theory the exponents are assumed
46 to be universal with theoretical 3D values of ~ 2 , a wide range of values have been reported
47 for rheological thresholds based on G' in polymer composites based on carbon nanotubes:
48 0.70,¹² 2.91,³¹ 2.64 and 2.59,³² which suggests that G' or G'/G'' follow different scaling
49 laws to describe their volume fraction dependence when compared with electrical conducting
50 σ .³²
51
52
53
54
55
56
57
58
59
60

CONCLUSIONS

Two different CNFs were incorporated in in the same polypropylene (PP) matrix by twin-screw extrusion under the same processing conditions. Electrically, the two carbon nanofiber based polypropylene composites demonstrated to have different response: non-conducting and conducting as a function of volume fraction concentration. A large difference in the rheological behavior of both composites has been measured. Whereas the electrical conducting composites based on PR 24 LHT XT carbon nanofibers show liquid-like to solid-like transition which leads to the plateaus for G' , G'' at low frequencies, the electrical isolating composites based on PR 25 PS XT carbon nanofibers remain practically unaltered in their rheological behavior when compared to the pure PP composites. This fact suggests that rheological analysis clearly differentiates electrical conducting from insulating performance for this particular type of systems. Furthermore, after comparing electrical conductivity and rheological analysis, it is concluded that G' / G'' and in less extent G' are the most appropriate rheological parameters for comparing with electrical behavior, which is consistent with previous works that identify elastic load rheological parameters as the best candidates to compare to the onset of electrical percolation. The rheological threshold fitted from G' / G'' was found to be ~ 0.5 % vol, slightly higher than electrical percolation threshold ~ 0.4 % vol. Finally, the difference found between exponents in G' / G'' and G' fittings, suggests different scaling laws to describe their volume fraction dependence when compared with electrical conductivity σ .

ACKNOWLEDGMENTS

Financial support for this work has been provided by Consellería de Educación e Ordenación Universitaria, Xunta de Galicia through grant CN2011/008.

REFERENCES AND NOTES

- 1
2
3
4
5
6
7
8
9
10
11
12
13
14
15
16
17
18
19
20
21
22
23
24
25
26
27
28
29
30
31
32
33
34
35
36
37
38
39
40
41
42
43
44
45
46
47
48
49
50
51
52
53
54
55
56
57
58
59
60
- 1 Kang, I.; Heung, Y.Y.; Kim, J.H.; Lee, J.W.; Gollapudi, R.; Subramaniam, S.;
Narasimhadevara, S.; Hurd, D.; Kirikera, G.R.; Shanov, V.; Schulz, M.J.; Shi, D.; Boerio, J.;
Mall, S.; Ruggles-Wren, M. *Compos. Part B-Eng.* **2006**, *37*, 382-394.
- 2 Burton, D.J.; Glasgow, D.G.; Lake, M.L.; Kwag, C.; Finegan, J.C.; In Repecka LSFF (ed)
A Materials and Processes Odyssey, Books 1 and 2, vol 46. International Sampe Technical
Conference Series **2001**; pp 647-657.
- 3 Gordeyev, S.A.; Macedo, F.J.; Ferreira, J.A.; van Hattum, F.W.J.; Bernardo, C.A. *Physica*
B. **2000**, *279*, 33-36.
- 4 Al-Saleh, M.H.; Sundararaj, U. *Carbon.* **2009**, *47*, 2-22.
- 5 Tibbetts, G.G.; Lake, M.L.; Strong, K.L.; Rice, B.P. *Compos. Sci. Technol.* **2007**, *67*,
1709-1718.
- 6 Das, N.C.; Yamazaki, S.; Hikosaka, M.; Chaki, T.K.; Khastgir, D.; Chakraborty, A. *Polym.*
Int. **2005**, *54*, 256-259.
- 7 Huang, J.C. *Adv. Polym. Tech.* **1995**, *14*, 137-150.
- 8 Lillehei, P.T.; Kim, J-W.; Gibbons, L.J.; Park, C. *Nanotechnology.* **2009**, *20*, 325708-
325714.
- 9 Gershon, A.L.; Cole, D.P.; Kota, A.K.; Bruck, H.A. *J. Mater. Sci.* **2010**, *45*, 6353-6364.
- 10 Schadler, L.S.; Giannaris, S.C.; Ajayan, P.M. *Appl. Phys. Lett.* **1998**, *73*, 3842-3844.
- 11 Fiedler, B.; Gojny, F.H.; Wichmann, M.H.G.; Nolte, M.C.M.; Schulte, K. *Compos. Sci.*
Technol. **2006**, *66*, 3115-3125.

1
2
3 12 Du, F.M.; Scogna, R.C.; Zhou, W.; Brand, S.; Fischer, J.E.; Winey, K.I. *Macromolecules*.
4
5 2004, 37, 9048-9055.
6

7
8 13 Wagener, R.; Reisinger, T.J.G. *Polymer*. 2003, 44, 7513-7518.
9

10
11 14 Kharchenko, S.B.; Douglas, J.F.; Obrzut, J.; Grulke, E.A.; Migler, K.B. *Nat. Mater.* 2004,
12 3, 564-568.
13

14
15 15 Kota, A.K.; Cipriano, B.H.; Duesterberg, M.K.; Gershon, A.L.; Powell, D.; Raghavan,
16 S.R.; Bruck, H. A. *Macromolecules*. 2007, 40, 7400-7406.
17

18
19 16 Zhu, J.; Wei, S.; Yadav, A.; Guo, Z. *Polymer*. 2010, 51, 2643-2651.
20

21
22 17 Evora, M.C.; Klosterman, D.; Lafdi, K.; Li, L.; Abot, J. L. *Carbon*. 2010, 48, 2037-2046.
23

24
25 18 Tessonier, J-P.; Rosenthal, D.; Hansen, T.W.; Hess, C.; Schuster, M.E.; Blume, R.;
26 Girgsdies, F.; Pfaender, N.; Timpe, O.; Su, D.S.; Schloegl, R. *Carbon*. 2009, 47, 1779-1798.
27

28
29 19 Paleo, A.J.; van Hattum, F.W.J.; Pereira, J.; Rocha, J.G.; Silva, J.; Sencadas, V.; Lanceros-
30 Mendez, S. *Smart. Mater. Struct.* 2010, 19, 065013-065019.
31

32
33 20 <http://www.apsci.com>
34

35
36 21 Bunde, A.; Havlin, S. In *Fractals and disordered systems*; Springer: New York, 1996; pp
37 27-8.
38

39
40 22 Heaney, M.B. *Phys. Rev. B*. 1995, 52, 12477-12480.
41

42
43 23 Garboczi, E.J.; Snyder, K.A.; Douglas, J.F.; Thorpe, M.F. *Phys. Rev. E*. 1995, 52, 819-
44 828.
45

46
47 24 Kalaitzidou, K.; Fukushima, H.; Askeland, P.; Drzal, L. T. *J. Mater. Sci.* 2008, 43, 2895-
48 2907.
49

- 1
2
3 25 Mutel, M.R.K. Utracki, L.A., Ed.; Carl Hanser: Munich, 1991, Chapter 12.
4
5
6 26 Ferry, J.D. In *Viscoelastic Properties of Polymers*; Wiley: New York, 1980.
7
8
9 27 Potschke, P.; Fornes, T.D.; Paul, D.R. *Polymer*. 2002, 43, 3247-3255.
10
11
12 28 Utracki, L.A. *Polym. Composite*. 1986, 7, 274-282.
13
14
15 29 Lozano, K.; Yang, S.Y.; Zeng, Q. *J. Appl. Polym. Sci*. 2004, 93, 155-162.
16
17
18 30 Cipiriano, B.H.; Kashiwagi, T.; Raghavan, S.R.; Yang, Y.; Grulke, E.A.; Yamamoto, K.;
19
20 Shields, J.R.; Douglas, J.F. *Polymer*. 2007, 48, 6086-6096.
21
22
23 31 Martins, J.N.; Bassani, T.S.; Barra, G.M.O.; Oliveira, R.V.B. *Polym. Int*. 2011, 60, 430-
24
25 435.
26
27
28 32 Huang, C.L.; Wang, C. *Carbon*. 2011, 49, 2334-2344.
29
30
31
32
33
34
35
36
37
38
39
40
41
42
43
44
45
46
47
48
49
50
51
52
53
54
55
56
57
58
59
60

1
2
3 **FIGURE 1** SEM micrographs of 1.9 % vol PP / CNFs composites: (a) PP / PR 24 LHT XT
4 composites, (b) PP / PR 25 PS XT composites.
5
6

7 **FIGURE 2** Electrical conductivity values versus volume fraction loadings of CNFs and
8 corresponding fit using equation 1. R^2 is 0.99 for the PP/ PR 24 LHT XT composites fitting.
9
10

11 **FIGURE 3** Storage moduli of (a) PP / PR24LHTXT composites and (b) PP / PR25PSXT
12 composites as a function of frequency at 190 ° C.
13
14

15 **FIGURE 4** Loss moduli of (a) PP / PR24LHTXT composites and (b) PP / PR25PSXT
16 composites as a function of frequency at 190 ° C.
17
18

19 **FIGURE 5** Inverse loss tangent of (a) PP / PR24LHTXT composites and (b) PP / PR25PSXT
20 composites as a function of frequency at 190 ° C.
21
22

23 **FIGURE 6** Complex viscosity of (a) PP / PR24LHTXT composites and (b) PP / PR25PSXT
24 composites as a function of frequency at 190 ° C.
25
26

27 **FIGURE 7** The normalized log values of electrical conductivity σ , storage modulus G' , loss
28 modulus G'' , inverse loss tangent G' / G'' and complex viscosity η^* as a function of
29 PR24LHTXT's concentration. The rheological data corresponds to a frequency of 0.1 rad/s.
30 The dashed line is to guide the eyes.
31
32
33
34
35
36

37 **Table 1.** Composites' nomenclature
38

39 **Table 2.** Fitting results for power-law relations in electrical and rheological experiences for
40 PP / PR 24 LHT XT composites
41
42
43
44
45
46
47
48
49
50
51
52
53
54
55
56
57
58
59
60

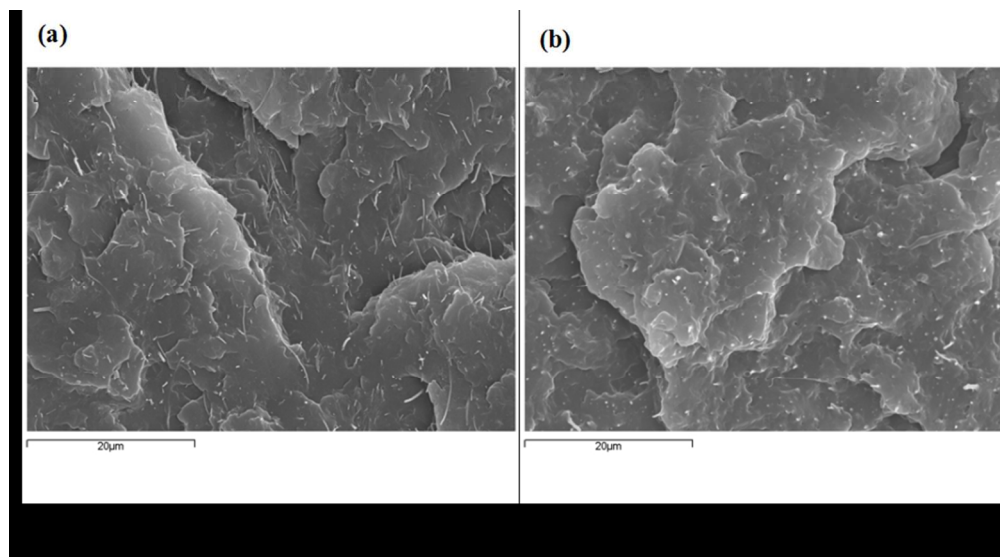


FIGURE 1 SEM micrographs of 1.9 % vol PP / CNFs composites: (a) PP / PR 24 LHT XT composites, (b) PP / PR 25 PS XT composites.
163x90mm (150 x 150 DPI)

er Review

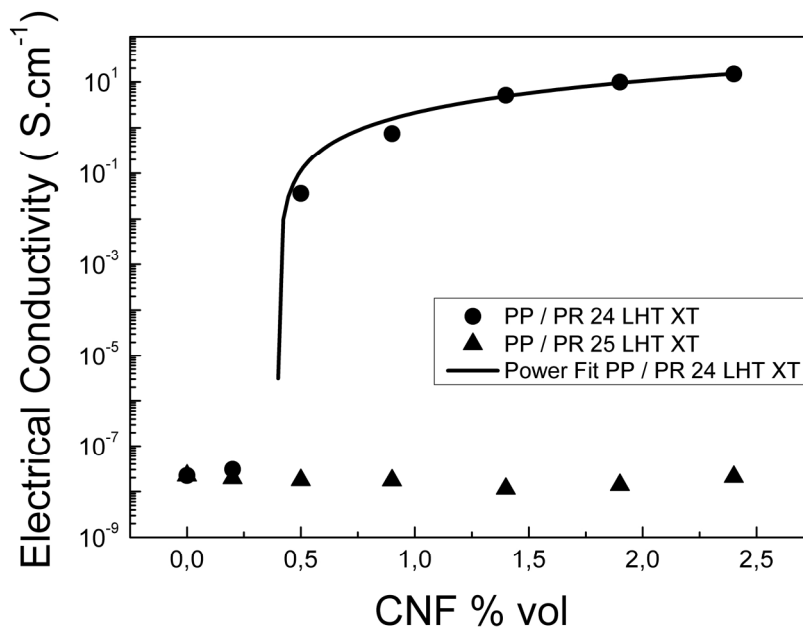
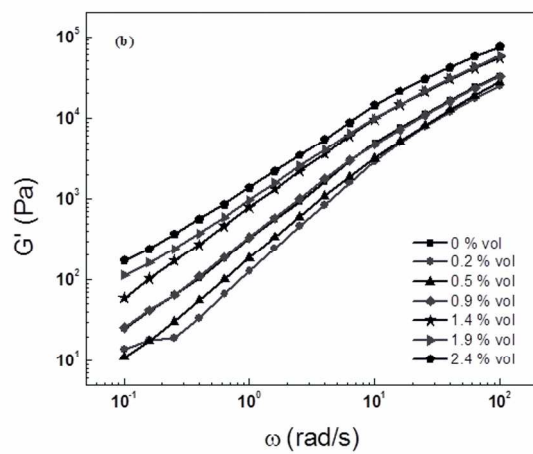
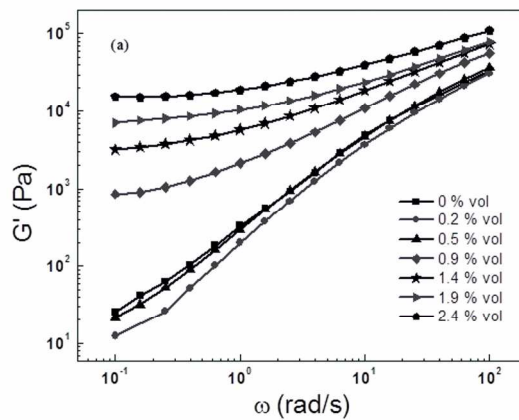


FIGURE 2 Electrical conductivity values versus volume fraction loadings of CNFs and corresponding fit using equation 1. R2 is 0.99 for the PP/ PR 24 LHT XT composites fitting.
202x141mm (300 x 300 DPI)



42
43
44
45
46
47
48
49
50
51
52
53
54
55
56
57
58
59
60

FIGURE 3 Storage moduli of (a) PP / PR24LHTXT composites and (b) PP / PR25PSXT composites as a function of frequency at 190 ° C. 163x172mm (300 x 300 DPI)

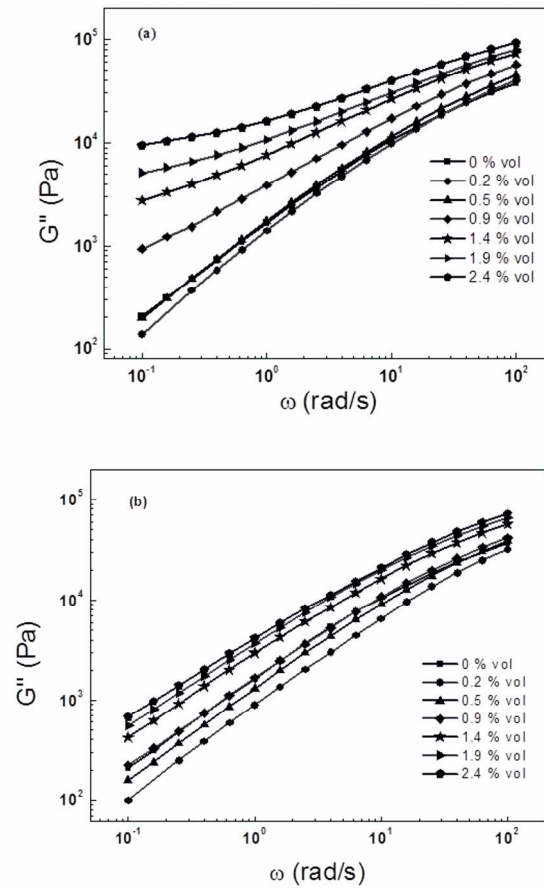


FIGURE 4 Loss moduli of (a) PP / PR24LHTXT composites and (b) PP / PR25PSXT composites as a function of frequency at 190 °C.
163x174mm (300 x 300 DPI)

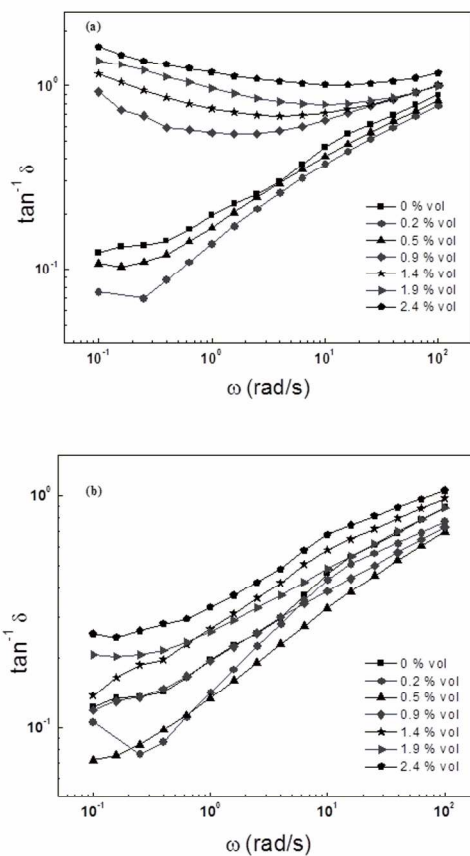


FIGURE 5 Inverse loss tangent of (a) PP / PR24LHTXT composites and (b) PP / PR25PSXT composites as a function of frequency at 190 ° C.
163x171mm (300 x 300 DPI)

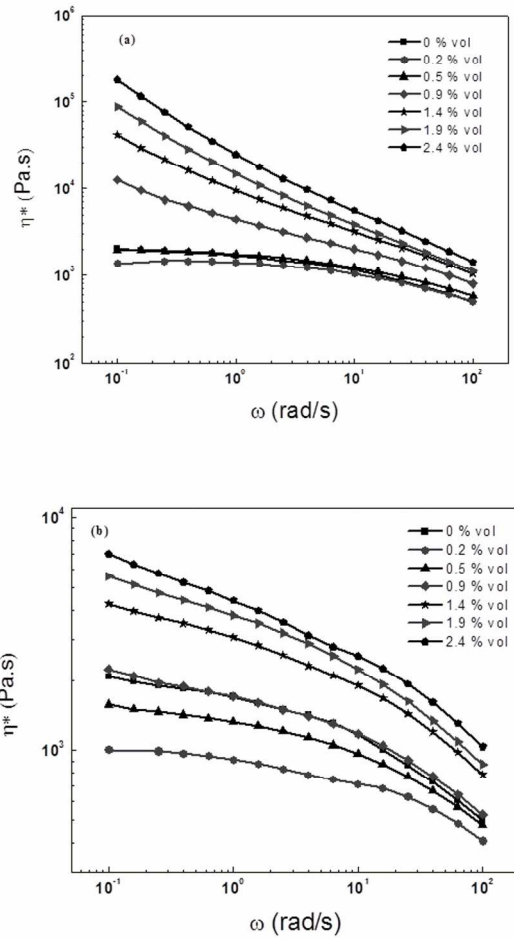


FIGURE 6 Complex viscosity of (a) PP / PR24LHTXT composites and (b) PP / PR25PSXT composites as a function of frequency at 190 ° C.
163x183mm (300 x 300 DPI)

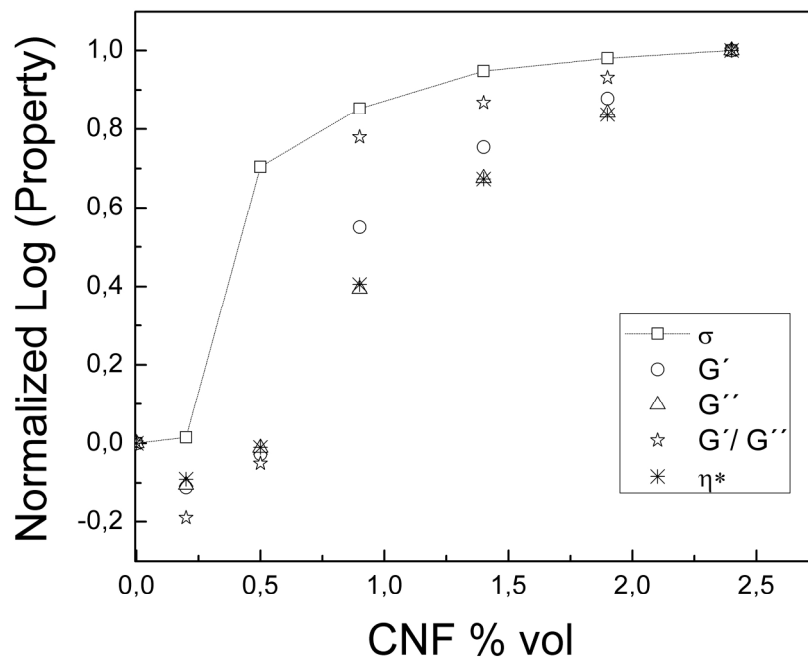


FIGURE 7 The normalized log values of electrical conductivity σ , storage modulus G' , loss modulus G'' , inverse loss tangent G'/G'' and complex viscosity η^* as a function of PR24LHTXT's concentration. The rheological data corresponds to a frequency of 0.1 rad/s. The dashed line is to guide the eyes.
221x169mm (300 x 300 DPI)

Table 1. Composites' Nomenclature

Composite Nr	CNF type	CNF grade	Polypropylene	CNFs Loadings
1	PR24	LHT XT	Borealis EE002AE	0.2, 0.5, 0.9, 1.4, 1.9, 2.4 % vol
2	PR25	PS XT		

For Peer Review

Table 2. Fitting results for power-law relations in electrical and rheological experiences

Power-law relation	Percolation threshold, ϕ_c (vol %)	t	R2
$\sigma \propto (\phi - \phi_c, \sigma)^t$	0.42	1.75	0.99
$G'/G'' \propto (\phi - \phi_c, G'/G'')^t$	0.49	0.52	0.99
$G' \propto (\phi - \phi_c, G')^t$	0.47	1.54	0.99

For Peer Review